Fluid Phase Equilibria 269 (2008) 73–79

Contents lists available at ScienceDirect

Fluid Phase Equilibria

journal homepage: www.elsevier.com/locate/fluid

Prediction of Henry's constants of xenon in *cyclo*-alkanes from molecular dynamics simulations

Huajun Yuan[a], Cynthia J. Jameson[a], Sumnesh K. Gupta[b], James D. Olson[a], Sohail Murad[a,*]

[a] *Department of Chemical Engineering, University of Illinois at Chicago, 810 S. Clinton, Chicago, IL 60607, United States*
[b] *The Dow Chemical Company, 770 Building, South Charleston, West Virginia 25303, 1400 Building Midland, MI 48667, United States*

ARTICLE INFO

Article history:
Received 21 February 2008
Received in revised form 6 May 2008
Accepted 8 May 2008
Available online 16 May 2008

Keywords:
NMR
Intermolecular interactions
Gas solubility
Henry's constant

ABSTRACT

Using the molecular dynamics (MD) method, we demonstrate that intermolecular nuclear magnetic resonance (NMR) chemical shifts can be used to evaluate and develop intermolecular potentials for cross-interactions for use in solubility studies. The calculation of chemical shifts in MD is an order of magnitude more efficient than solubilities, which makes it an attractive tool for fine-tuning potential models. We examine the average Xe chemical shifts in *cyclo*-alkanes over a range of temperatures to develop a suitable potential model for the cross-interactions between Xe and a series of *cyclo*-alkanes. Our results clearly demonstrate that potential models that show better agreement with experiments for chemical shift, invariably lead to better agreement with experiment for Henry's constant and solubility of gases in solvents.

1. Introduction

Safety standards for storage of flammable liquids require precise knowledge of the amount of O_2 dissolved. Experimental studies often pose serious safety risks, especially under some extreme conditions. Molecular modeling is therefore a safe alternative to obtain such data provided that the methods and parameters of molecular level modeling can be validated experimentally [1]. Xenon is a suitable surrogate for O_2 for solubility studies. In the temperature range where experimental data are available for O_2 and Xe, previous studies have shown that molecular dynamics simulations provide accurate values of Henry's constants and gas solubility for O_2 and Xe if we use the same cross-interaction parameter for size in modifying the Lorenz–Berthelot mixing rules [2,3]. Cross parameters for size have also been found to be transferable for similar non-polar components such as other rare gas atoms and small non-polar molecules such as O_2, N_2, and CH_4 as well [4,5]. A series of closely related non-polar liquids whose molecular structures and properties are well known can therefore serve as prototype systems to aid understanding of gas–liquid solubility. We have investigated solvents in the same homologous series in this study, where they differ from each other in a systematic way, for example, by a CH_2 group. This approach also allows group contribution methods to be examined as predictive tools. The interactions between Xe and *n*-alkanes, in particular has been extensively studied [6–9]. It will be of interest to investigate the interaction between Xe and *cyclo*-alkanes to gain better insight on the role of solvent structure on gas solubilites.

For a solute in a liquid solvent, the average chemical shift depends on the free volume associated with the liquid structure of the solvent and the solute–solvent intermolecular interactions [10]. Herein lies the connection between the average chemical shifts and intermolecular interactions, since the solubility depends primarily on the same factors. Therefore, a solute–solvent potential that gives improved chemical shift values can also be expected to lead to improved solubility values. In addition, accurate calculations of chemical shift require only local equilibrium, while solubilities require global equilibrium. Chemical shift can therefore be estimated relatively rapidly in molecular simulations, and provides a very accurate means of fine-tuning a potential that can be subsequently used for solubility studies.

The most widely used method for studying phase equilibrium (using molecular simulation) is by using Monte-Carlo (MC) methods such as the Gibbs ensemble Monte-Carlo [11]. A common problem with these techniques is that they become increasingly inefficient at higher densities because of the particle insertions that must be carried out. Several methods have recently been suggested that circumvent this problem to some degree [12]. However, some of the methods do not work well at the low concentrations that must be studied when gases dissolve in a liquid [13]. We present a method that allows gas solubility to be obtained in a rather straightforward manner in a simulation that is strikingly close to actual

* Corresponding author. Tel.: +1 312 996 5593.
E-mail address: murad@uic.edu (S. Murad).

0378-3812/$ – see front matter © 2008 Elsevier B.V. All rights reserved.
doi:10.1016/j.fluid.2008.05.003

Table 1
Coefficients for site-site isotropic chemical shift functions used in this work, as defined in Eq. (1) [14]

	N				
	6	8	10	12	14
Xe–C(H_n)c_n (Å^{-n})	-1.48211×10^5	1.045×10^7	-1.90132×10^8	1.38433×10^9	-3.45561×10^9
Xe–H h_n (Å^{-n})	8.58334×10^3	6.55733×10^5	1.42131×10^7	-6.34747×10^7	4.20088×10^7

experiments. In addition, since the method is based on the molecular dynamics, dynamic properties such as diffusion coefficients can also be obtained easily if needed.

In recent MD simulations on *n*-alkanes, we have used both rigid and flexible models for the solvent [9]. In our current study, as a follow up, we attempt to answer the following questions: when the solvent changes to *cyclo*-alkanes (which have cyclic ring instead of linear chain configuration), what is the magnitude of change in the solvent configuration? Is the potential used for the linear alkanes still applicable? Can we still get good solubility estimates using the linear alkane potential? To answer these questions, we need to compare our studies directly with our previous work by using exactly the same chemical shift functions, and the same potential functions for Xe–C, Xe–H.

The objective of this paper is to develop a description of Xe in liquid *cyclo*-alkanes that can lead to accurate values for the solubility. We have already established that the Xe chemical shift reaches a converged average value in a fraction of the MD steps that are required to reach a converged value of the solubility [10]. Therefore, we will use the Xe chemical shift to develop and validate our models for the liquid structure and the Xe–liquid interactions.

To understand the intermolecular interactions between Xe and *cyclo*-alkanes, we investigate the Xe chemical shifts in *cyclo*-alkanes. To validate the potential model, we also investigate the variation of the Xe chemical shifts with the number of carbons in the solvent molecule at corresponding thermodynamic states of the liquids, i.e., at the same reduced temperature. Finally, we compare the CH_2 contributions in *n*-alkanes and in *cyclo*-alkanes. All the solvents considered in the present work are *cyclo* (cyclic ring) hydrocarbons.

2. Methods

2.1. Chemical shift and potential functions

As discussed in a previous study by Jameson et al. [14], the Xe chemical shift function is expressed as

$$\delta = \sum_{H(j)}\sum_{n=6}^{14} h_n r_{\mathrm{Xe-H}(j)}^{-n} + \sum_{C(k)}\sum_{n=6}^{14} c_n r_{\mathrm{Xe-C}(k)}^{-n} \quad (1)$$

where h_n and c_n are chemical shift coefficients for Xe–H and Xe–C and are listed in Table 1. $r_{\mathrm{Xe-H}(j)}$ is the distance between a Xe atom and the *j*th H atom in the alkane, while $r_{\mathrm{Xe-C}(k)}$ is the corresponding distance for Xe–C. For the MD simulations in the *cyclo*-alkanes in this work, a flexible all atom (AA) model was chosen to represent the cyclic molecules of interest. The solvent–solvent intermolecular interactions are described by the pairwise Lennard–Jones potential:

$$u_{ij} = \sum_i^a \sum_j^b 4\varepsilon_{ij}\left[\left(\frac{r_{ij}}{\sigma_{ij}}\right)^{-12} - \left(\frac{r_{ij}}{\sigma_{ij}}\right)^{-6}\right] \quad (2)$$

where r_{ij} is the distance between two interacting sites *i* and *j*, while the potential parameters ε_{ij} and σ_{ij} for these interactions were taken from Gianni [15,16] and Milano and Muller-Plathe [17], as listed in Table 2. For the solvent potential functions we needed to use a set of parameters which are appropriate for *cyclo*-alkanes rather than simply using the same set from Jorgensen et al. [18], the set which is now in standard use for linear alkanes, and which we used for previous study (literature [9] our linear alkane paper) It was already clear from their original paper that simulations of liquid *cyclo*-hexane using the final set of parameters gave results that are not in good agreement with the experimental properties (density, enthalpy of vaporization) used for testing. This is not surprising, particularly the torsion parameters in cyclic systems can not be the same as in linear chains; there is more restricted rotation about the C–C bonds in the cyclic alkanes. The potential parameters used by the Muller-Plathe group for cyclic hydrocarbons give more accurate thermodynamic properties (including liquid densities) and they also used other properties such as diffusion coefficient, reorientation times in pure solvents as well as in mixtures [17,19] so we adopted these in Table 2. Combining rules for interactions between different species are prescribed by the geometric mean. The intermolecular potential parameter of pure Xenon was also taken from literature [20]. We use exp-6 functions to describe the Xe–C and Xe–H interactions [14] since The Lennard–Jones potential is usually not adequate for this purpose: the r^{-12} form is too steep and for gas solubilities, having the correct repulsive interaction is rather important since the solute molecules sample this region frequently:

$$u_{\mathrm{Xe}-i} = \sum_i \varepsilon_{\mathrm{Xe}-i}\left\{\left(\frac{6}{\alpha_{\mathrm{Xe}-i}-6}\right) \times \exp[\alpha_{\mathrm{Xe}-i}(1-\bar{r})] - \left(\frac{\alpha_{\mathrm{Xe}-i}}{\alpha_{\mathrm{Xe}-i}-6}\right)\bar{r}^{-6}\right\} \quad (3)$$

where $\bar{r} = r_{\mathrm{Xe}-i}/r_{\mathrm{min,Xe}-i}$. The parameters ε, α and r_{min} for Xe–C_{alkyl}, Xe–H_{alkyl} are given in Table 2.

Table 2
Flexible all atom potential parameters for *cyclo*-alkanes [14] and parameters for Xe–*Cyclo*-alkane interactions, as defined in Eq. (2)

Atom type		ε (kcal/mol)		σ (Å)		q (e$^-$)
H		0.0452		2.58		0.0
C		0.0715		3.28		0.0
Bond stretching			Angle bending: $u = k\theta(\theta-\theta_0)2$			
Type	R_0 (Å)	K_r (kcal/mol)	Type	θ_0 (°)	k_θ (kcal/(mol rad^2))	
C–C	1.526	268	H–C–H	109.5	34.69	
C–H	1.090	340	H–C–C	109.5	40.07	
			C–C–C	109.5	50.24	
Torsion: $u = k_\tau(1+\cos 3\varphi)/2$						
Type					k_τ (kcal/mol)	
C–C–C–C					2.4	
			Xe–*cyclo*-alkane interaction parameters			
			ε/k_B	α	r_{min} (Å)	
n-Alkanes [9] set A	Xe–C		141.2	16.1	3.75	
	Xe–H		53.3	15.9	3.44	
Modified, set B	Xe–C		141.2	16.1	3.99	
	Xe–H		53.3	15.9	3.66	

2.2. Henry's constant

During the simulation, we obtain the solubility of xenon in *cyclo*-alkanes from the Henry's constant via the equation [21]:

$$H_{12}(T, P_2^{\text{sat}}) = \lim_{x_1 \to 0} \left\{ \frac{P_1 \phi_1}{x_1 \exp\{(P_2 - P_2^{\text{sat}})\bar{V}_1^{\infty}/RT\}} \right\} \quad (4)$$

Eq. (4) includes contributions from the gas phase non-ideality as well as solvent pressure. The pressure (P_1) of the Xe gas phase is estimated from the density (ρ) of the gas phase and the second virial coefficient B using

$$P = (1 + B\rho)\rho RT \quad (5)$$

The vapor phase fugacity coefficients (ϕ) can similarly be obtained using

$$\ln \phi = 2\rho B - \ln\left(\frac{P}{\rho RT}\right) \quad (6)$$

The pressure in the solvent compartment (P_2) is calculated from the force on the membranes separating the two compartments in the simulation box, which represents the pressure difference between the two compartments. For xenon the second virial coefficient for our potential model was used which agreed well with experimental values reported in literature [22] and V_1^{∞} (partial molar volume of the gas dissolved at infinite dilution) can be calculated by performing a few additional simulations (at least one) and using Eq. (4).

2.3. Molecular dynamics

The MD methodology has been described in previous publications [23], so we will only summarize it here. The simulation box consists of a solvent/solution compartment separated from the gas compartment by a semi-permeable membrane. A schematic diagram of the simulations system is shown in Fig. 1. The membrane atoms are fixed at their equilibrium positions in an FCC structure. The system is made longer in the x direction (perpendicular to the membranes), $L_x = 4L_y = 4L_z$, to minimize the overall effect of the membranes. The membrane allows only the gas molecules (Xe) to freely permeate it, to enter the solution compartment, but prevents the solvent molecules (*cyclo*-alkanes) from moving to the gas compartment via the membrane.

The density of the solvent compartment can be fixed to correspond to the experimental value at the state condition (which agree with the values predicted by the models used here, see Section 2.1) of interest. In the studies carried out the variation of density with temperature was accounted for. This fixes the volume of the solvent compartment once the number of molecules to be included in the solvent compartment is specified. Typically the solvent compartment consisted of 480 molecules and the two membranes consisted of 128 atoms. In some simulations, some gas molecules were also included in the solvent compartment to facilitate the approach to equilibrium. For convenience, the volume of the gas compartment has been set at half of the solvent compartment. The initial number of Xe molecules in the gas compartment is determined by the desired initial pressure of Xe. In general, in our studies we included up to 60 Xe atoms. Since the total number of *cyclo*-alkane molecules in the solution compartment remains fixed during the simulation (the membrane is impermeable to *cyclo*-alkanes) and are at least an order of magnitude larger than the number of Xe atoms in this compartment, the liquid density in the solution compartment remains essentially constant.

The time evolution of this initial system is studied with a velocity Verlet algorithm, using the LAMMPS code [24]. The initial parameter set was taken from the flexible all atom force field, for *cyclo*-pentane, *cyclo*-hexane and *cyclo*-octane [15–17]. The Xe–C and Xe–H potential parameters used in our previous work [9] (set A in Table 2) were also used in this work. As will be described in the next section, these were adjusted to improve agreement with experimental values of chemical shift. The original (set A) and modified (set B) potential parameters are given in Table 2. The temperature was held constant using a Nose/Hoover thermostat. The solvent in the solution compartment was annealed at 750 K to get a uniform density distribution. After this, production runs

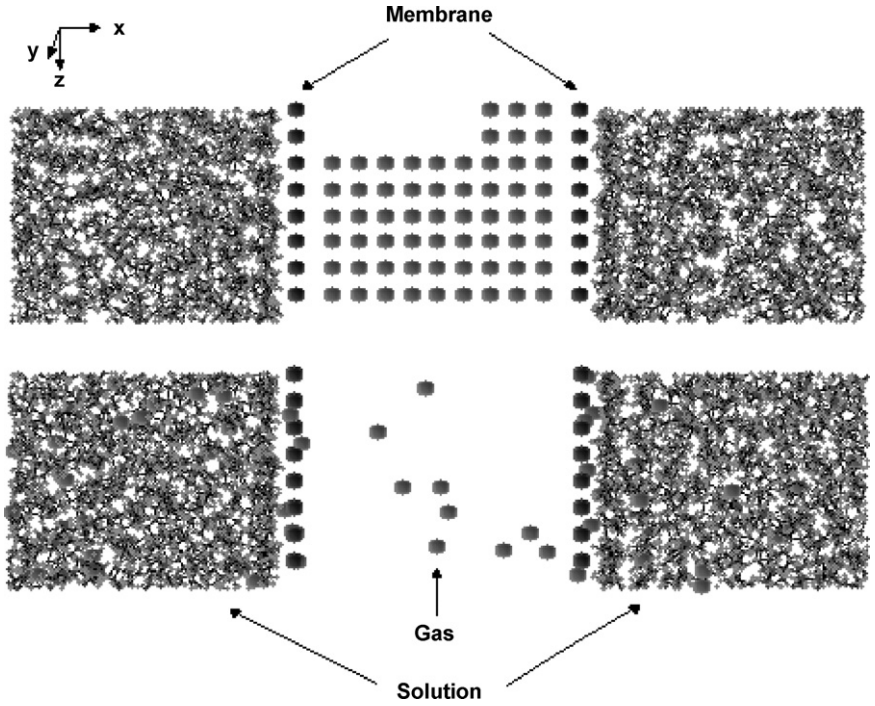

Fig. 1. Simulation system for investigating chemical shift and solubility of gas dissolved in liquids, at the beginning of the simulation and after equilibration.

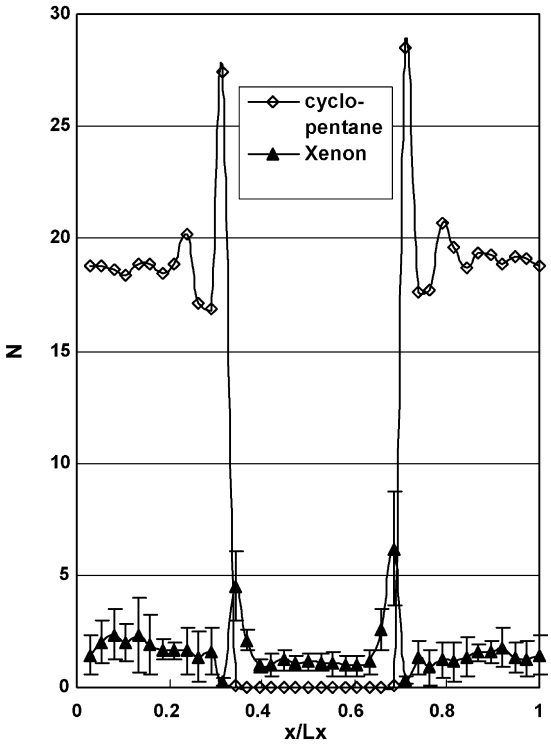

Fig. 2. The density profile of solvent and Xe at the end of a typical MD simulation with 4×10^6 steps.

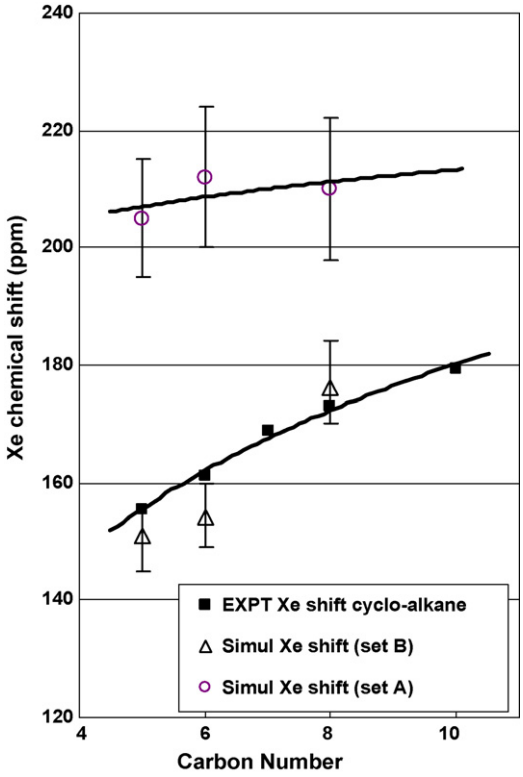

Fig. 3. Comparison between average Xe chemical shifts at 298 K, calculated using the set B Xe–alkane potential, the same as was used for the rigid *n*-alkane model (from literature [14]) and using the set A Xe–alkane potential, the same as was used for the flexible *n*-alkane model (from literature [9]). The experimental values are from literature [25].

were carried out for 2×10^6 to 5×10^6 time steps, of size 1×10^{-16} s. Properties of the system such as Xe chemical shift, gas pressure, liquid/gas concentrations were calculated during the production run. A typical density profile from a simulation is shown in Fig. 2. The density profile can then be used to estimate both the pressures of the gas and solution compartments, and the solubility of the Xe in *cyclo*-alkanes. Using Eq. (4) Henry's constant can then be calculated.

3. Results and discussion

3.1. Modifications of solute–solvent potential by chemical shift calculation

In our investigations we first carried out simulations to estimate chemical shifts using our previously developed Xe–*n*-alkane chemical shift and intermolecular potential functions (Eqs. (1) and (3)). We were interested in determining whether the same Xe–CH_2 potential function is able to reproduce the experimental chemical shifts in both cyclic and linear alkanes using similar parameters. In Fig. 3, the comparison of the MD results at 298 K with experimental values of *cyclo*-pentane clearly indicate that the chemical shifts relative to the reference (free Xe atom at 0 ppm) have the correct sign but are off by 15–30%. As seen in Table 3, the set A Xe–*n*-alkane potential found in literature [9] gives similar systematically larger chemical shifts for all three *cyclo*-alkanes. Because the Xe chemical shift average converges rapidly, we were able to adjust the potential parameters relatively easily (r_{min} only) to set B (incidentally, the same as that which had been found in literature [14] for rigid *n*-alkanes) which improves the agreement with experiment. That is, we found the chemical shift values of *cyclo*-alkanes to be similar for rigid and flexible models, unlike in *n*-alkanes [9]. The number of stable molecular conformations is smaller for *cyclo*-alkanes than for *n*-alkanes. For example, the chair inversion process in cyclohexane is a rare event near a Xe molecule. This has also been noted by Luhmer and Bartik [25]. The Xe atom therefore sees the cyclohexane molecule, to some extent as a semi-rigid molecule. Modifying the r_{min} for Xe–C and Xe–H in *cyclo*-alkanes to be more like that which apply to rigid models was therefore a reasonable direction for adjustment. Such an adjustment with a shorter r_{min} for (the potential for Xe–C and Xe–H) linear than cyclo alkanes is also con-

Table 3
Comparison of average Xe chemical shifts (ppm) and Henry's constant (atm) at 298 K calculated using the set A Xe–alkane potential, compared with the modified set B Xe–alkane model

Number of carbons	Chemical shift (ppm)			Henry's constant (atm)		
	Using set A	Using set B	Expt [25]	Using set A	Using set B	Expt[a]
5	205	151	155.5	65.7 ± 10	56.0 ± 8	47.9 ± 9
6	212	154	161.1	64.1 ± 12	53.1 ± 6	48.8 ± 9
7			168.69			
8	210	176.1	173.12	65.0 ± 12	60.1 ± 8	48.8 ± 9
10			179.48			

[a] Estimated from solubility at 1 atm from literature [28].

Table 4
Xe chemical shifts (ppm) in *cyclo*-alkanes at $T^* = 0.5$, calculated using the modified set B exp-6 potential

	Cyclo-pentane	*Cyclo*-hexane	*Cyclo*-octane
T_c (K)	512	554	648
T (K)	256	277	324
Calculated	153 ± 8	150 ± 6	153 ± 6

sistent with parameters obtained for equations of state often used to estimate solubility [26].

3.2. Further validation of potential models

Since chemical shifts can be obtained rather efficiently we further tested our potential models by examining additional characteristics of the chemical shift and comparing them to their known theoretical and experimental characteristics. The final MD values for the average Xe chemical shifts in various liquids at 298 K are given in Table 3. As noted earlier the agreement with experimental values is very good. We have also estimated the values of chemical shift at T^* ($=T/T_c$) = 0.5 for Xe in *cyclo*-pentane, *cyclo*-hexane and *cyclo*-octane in Table 4. We find these to be very similar values, when the same thermodynamic states are compared, there is essentially no dependence of the observed Xe chemical shift in the various *cyclo*-alkane solvents on the number of carbons. As we did for the linear alkanes [9], we compare the effective second virial coefficient of the Xe chemical shift in the solvent, $\delta_{1\text{effective}}$, obtained by dividing the observed Xe chemical shift in solution relative to the Xe atom by the density of the liquid. We find that the contributions to $\delta_{1\text{effective}}$ are nearly constant (at $T^* = 0.5$) for the *cyclo*-alkanes, and similar behavior is observed in the linear alkanes; in Table 5, the $\delta_{1\text{effective}}$ (Xe–CH_2), the per CH_2 contribution at $T^* = 0.5$ are found to be very similar for the three *cyclo*-alkanes. However, there is a significant difference between linear and *cyclo*-alkanes. The $\delta_{1\text{effective}}$ (Xe–CH_2) (~2.69 ppm mol^{-1} L^{-1} per CH_2) is smaller than the corresponding values (~3.14 ppm mol^{-1} L^{-1} per CH_2) found in the linear alkanes.

These results illustrate the dependence of the Xe chemical shfit on the accessibility of the atoms providing electronic response which gives rise to the chemical shift. End groups have a distinct advantage in contributing to the Xe chemical shift because of the site effect. Likewise, we should expect that the constraints associated with the cyclic geometry will keep the CH_2 from getting as close to the Xe atom as does the CH_2 in a linear chain; the CH_2 groups in a linear alkyl chain are more exposed to Xe than the CH_2 groups in *cyclo*-alkanes. This is clearly seen in the ~3.14 ppm mol^{-1} L^{-1} per CH_2 for the linear alkanes compared to the ~2.69 ppm mol^{-1} L^{-1} per CH_2 for the *cyclo*-alkanes. This further validates that the potential parameters for the solute–solvent cannot be expected to be transferable between these two types of alkanes.

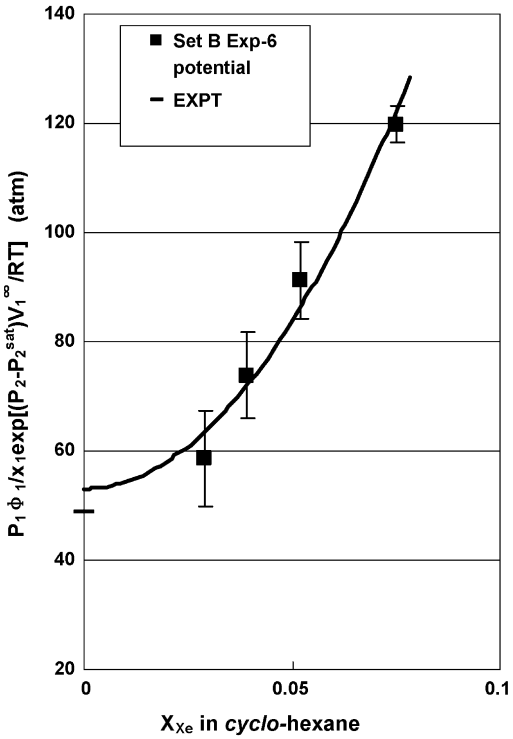

Fig. 4. Calculation of Henry's constant using modified (set B) potential model for Xe in *cyclo*-hexane. The curves extrapolate to the limiting value at zero mole fraction. The experimental value is from literature [27].

3.3. Solubility and Henry's constant

The results for the calculations of the solubilities of Xe in the various *cyclo*-alkanes are shown in Table 3, where the results using the original potential and the modified potential are compared with experimental values. A range of mole fractions of Xe in solution were investigated starting with various initial Xe gas pressures. Henry's constant was then obtained by extrapolation of the results to zero mole fraction, as shown in Fig. 4.

From the results for *cyclo*-pentane shown in Table 3 we see that there is systematic improvement in the calculated values of the Henry's constant when the modified exp-6 potential is used (see Table 3). The experimental value of Henry's constant is approximately 47.9 ± 9 atm (estimated from the solubility at 1 atm). The set A potential model (not fitted to the chemical shift) gives an extrap-

Table 5
Constitutive contributions to Xe chemical shift (ppm) and $\delta_{1\text{effective}}$(Xe–$CH_2$) (ppm mol^{-1} L^{-1}) for Xe in *n*-alkanes and *cyclo*-alkanes

	$T = 298$ K[a]			$T^* = 0.5$[a]		
	5[b]	6[b]	8[b]	5[b]	6[b]	8[b]
Cyclo-alkanes	*Cyclo*-pentane	*Cyclo*-hexane	*Cyclo*-octane	*Cyclo*-pentane	*Cyclo*-hexane	*Cyclo*-octane
CH_2 contribution (ppm)	30.2	25.7	22	30.6	25.0	19.1
$\delta_{1\text{effective}}$ (Xe–CH_2) ((ppm mol^{-1} L^{-1}))	2.822	2.822	3.002	2.778	2.666	2.643
n-Alkanes	*n*-Pentane	*n*-Hexane	*n*-Octane	*n*-Pentane	*n*-Hexane	*n*-Octane
CH_2 contribution[c] (ppm)	26	21.7	18.1	30.2	24.7	19.7
$\delta_{1\text{effective}}$ (Xe–CH_2)[c] (ppm mol^{-1} L^{-1})	2.934	2.800	3.002	3.069	3.002	3.270

[a] Solvent.
[b] No. of carbon.
[c] Literature [9].

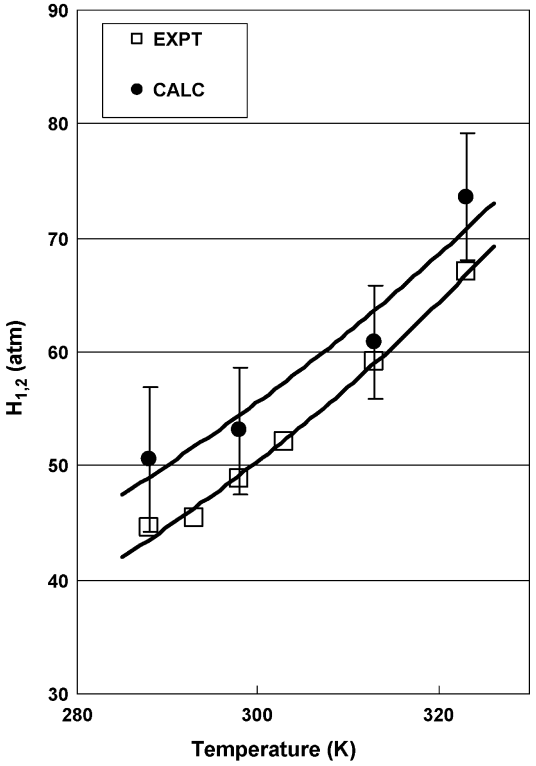

Fig. 5. Temperature dependence of Henry's constant for *cyclo*-hexane compared with experimental data from literature [25].

olated result of 65.7 ± 10, while for the set B potential (fitted to the chemical shift), the Henry's constant is 56.0 ± 8. Thus the modified potential leads to a significant improvement (beyond the experimental and simulation uncertainty). A similar improvement is seen for *cyclo*-hexane. The reported experimental value is 48.8 ± 7, while the extrapolated values from the original and modified potentials are 64.1 ± 12 and 53.1 ± 6, showing a significant improvement. For *cyclo*-octane the reported experimental value is 48.8 ± 7, while the extrapolated values from the set A and set B potentials are 65.0 ± 12 and 60.1 ± 8, once again showing a significant improvement. These improvements, while impressive, are not unexpected. The chemical shift is strongly dependent on the cross molecular interaction between the solute and solvents as is the Henry's constant. Most potentials currently available are fitted to vapor–liquid data that are not as sensitive to the cross-interactions.

A crucial and important test of a potential model is its ability to correctly estimate the temperature dependence of Henry's constant. This behavior is notoriously difficult to estimate theoretically and experimentally [1,3], because the behavior varies from substance to substance and depends on whether the enthalpy of solution of a solute in a solvent is positive or negative. For example, the Henry's constant of oxygen in benzene decreases as the temperature increases, while it increases in hexane in the temperature range 283–323 K [27,28]. The results for the temperature dependence of Henry's constant are shown for *cyclo*-hexane in Fig. 5. The results show the correct sign of the temperature coefficient and a reasonable agreement between the experimental temperature dependence, and the simulated values. This reinforces our belief, that potential models fitted to the chemical shift are more accurate for gas solubility and Henry's constants. A summary of all our results for Henry's constant for both models is given in Table 3. We also estimated the accuracy of the experimental measurements by fitting them to an equation of state [26] widely used for Henry's constants of such mixtures. Our results based on the observed deviations/scatter from the fitted data showed the experiments to be accurate to at least 5%.

4. Conclusions

We have investigated the Xe chemical shift in infinitely dilute solutions in *cyclo*-alkanes. The average intermolecular chemical shift of the solute is closely related to the local structure, and it converges in a fraction of the time necessary to obtain converged solubility. Our results show that potential parameters that lead to improved average chemical shifts do provide improved estimates for the solubility and Henry's law constants. This study has shown that the configuration of solvent molecules greatly influences the average Xe chemical shift. From our simulations we can separate out the mechanisms for the temperature dependence by looking at the effective second virial coefficient of the Xe chemical shift. The smaller second virial coefficient of Xe in *cyclo*-alkane suggests limited accessibility for the solute in the solvent, which in turn validates our modification of the solute–solvent potential parameters. We have shown that the solute–solvent potential which gives improved agreement with Xe chemical shifts do provide not only the correct magnitudes for Henry's constants but also the correct temperature dependence.

List of symbols

c_n	chemical shift coefficients for Xe–C (Å^{-n})
h_n	chemical shift coefficients for Xe–H (Å^{-n})
$H_{1,2}$	Henry's constant (atm)
k_θ	angular force constant (kcal/(mol rad^2))
k_τ	torsional force constant (kcal mol^{-1})
K_B	Boltzmann constant (J mol^{-1} K^{-1})
K_r	harmonic constant (kcal mol^{-1})
L	length of simulation system (Å)
P_1	pressure of gas phase (atm)
P_2^{sat}	vapor pressure of liquid (atm)
r_0	bond length (Å)
r_{i-j}	distance between two interacting sites i and j (Å)
r_{min}	exp-6 potential parameter (Å)
R	gas constant (J mol^{-1} K^{-1})
T	absolute temperature (K)
T_c	critical temperature (K)
T^*	reduced temperature, T/T_c
u_{Xe-I}	exp-6 potential parameter (kcal mol^{-1})
$\bar{V}_1^\infty$	partial molar volume of the solute at infinite dilution (cm^3 mol^{-1})
x_1	mole fraction of gas (1) in liquid (2)

Greek letters

α	exp-6 potential parameter
$\delta_{1effective}$	effective second virial coefficient (ppm/mol^{-1} L^{-1} per CH_2)
ε	LJ energy parameter (kcal mol^{-1})
θ_0	bond angle (°)
ρ	density (kg/m^3)
σ	LJ size parameter (Å)
φ	torsion angle (°)
ϕ	vapor phase fugacity coefficient

Acknowledgments

This research has been funded by the National Science Foundation [CBET-0730026 & CBET-0314203] and DOE [Grant No. DE-FG02-96ER14680 (SM)].

References

[1] S.K. Gupta, J.D. Olson, Ind. Eng. Chem. Res. 42 (2003) 6359–6374.
[2] M. Krishnamurthy, S. Murad, J.D. Olson, Mol. Simul. 32 (2006) 11–16.
[3] S. Murad, S. Gupta, Fluid Phase Equilib. 187 (2001) 29–37.
[4] R.P. Bonifacio, M.F. Costa Gomes, E.J.M. Filipe, Fluid Phase Equilib. 193 (2002) 41–51.
[5] G.L. Pollack, Science 251 (1991) 1323–1330.
[6] Y.H. Lim, A.D. King, J. Phys. Chem. 97 (1993) 12173–12177.
[7] Y.H. Lim, N. Nugara, A.D. King, J. Phys. Chem. 97 (1993) 8816–8819.
[8] Y.H. Lim, N. Nugara, A.D. King, Appl. Magn. Reson. 8 (1995) 521–531.
[9] H.J. Yuan, S. Murad, C.J. Jameson, J.D. Olson, J. Phys. Chem. 111 (2007) 15771–15783.
[10] C.J. Jameson, S. Murad, Chem. Phys. Lett. 380 (2003) 556–562.
[11] D.P. Landau, K. Binder, A Guide to Monte Carlo Simulations in Statistical Physics, 2nd Ed., Cambridge University Press, Cambridge, 2005.
[12] A.Z. Panagiotopoulos, J. Phys. Condens. Matter 12 (2000) 25–52.
[13] R.L. Rowley, M.W. Schuck, J.C. Perry, Mol. Phys. 86 (1995) 125–137.
[14] C.J. Jameson, D.N. Sears, S. Murad, J. Chem. Phys. 121 (2004) 9581–9592.
[15] C. Gianni, Chem. Phys. 189 (1994) 17–23.
[16] C. Gianni, Chem. Phys. 193 (1995) 101–108.
[17] G. Milano, F. Muller-Plathe, J. Phys. Chem. 108 (2004) 7415–7423.
[18] W.L. Jorgensen, D.S. Maxwell, J. Tirado-Rives, J. Am. Chem. Soc. 118 (1996) 11225–11236.
[19] R. Faller, H. Schmitz, O. Biermann, R.J. Muller-Plathe, Comput. Chem. 20 (1999) 1009–1017.
[20] M. Bohn, S. Lago, J. Fischer, F. Kohler, Fluid Phase Equilib. 23 (1985) 137–151.
[21] J.M. Prausnitz, R.N. Lichtenthaler, E. Gomes de Azevedo, Molecular Thermodynamics of Fluid Phase Equilibria, 3rd ed., Prentice Hall, New Jersey, 1986.
[22] J.H. Dymond, E.B. Smith, The Virial Coefficients of Gases: A Critical Compilation, Clarendon Press, Oxford, 1969.
[23] S. Murad, S.K. Gupta, Chem. Phys. Lett. 319 (2000) 60–64.
[24] LAMMPS (Large-scale Atomic/Molecular Massively Parallel Simulator) MD code developed by Steve Plimpton and co-workers at Sandia National Laboratories, DOE.
[25] M. Luhmer, K.J. Bartik, Phys. Chem. A. 101 (1997) 5278–5283.
[26] P.M. Mathias, Ind. Eng. Chem. Process Des. Dev. 22 (1983) 385–391.
[27] H.L. Clever, IUPAC Solubility Data Series, vol. 2, Pergamon Press, Oxford, 1979.
[28] G.L. Pollack, R.P. Kennan, J.F. Himm, P.W. Carr, J. Chem. Phys. 90 (1989) 6569–6579.